Journal of Bone Research
ISSN: 2572-4916

Research Article Open Access

Study of *In vitro* Bioactivity and Biodegradability of the Hydrothermally Prepared Carbon Nanofibrous/Hydroxyapatite (Cnf/Ha) Membranes

Abd El-Aziz A[1,2]*, Azza El-Maghraby[1] and Sherif H Kandil[2]

[1]*Department of Fabrication Technology, Advanced technology and New Materials Research Institute, Alexandria University, Egypt*
[2]*Department of Materials Science, Institute of Graduate Studies and Research, Alexandria University, Egypt*

Abstract

Critical size bone defects are orthopedic defects that will not heal without intervention or that will not completely heal over the natural life time of the animal. Although bone generally has the ability to regenerate completely however, critical defects need sort of scaffold to do so. In the current study, we proposed a method to get a Carbon NanoFibrous (CNFs) / Hydroxyapatite (HA) bioactive scaffold. The CNF nonwoven fabrics were obtained by the use of the electrospinning process of the polymeric solution of Poly Acrylonitrile (PAN) and next thermal treatment of both stabilization and carbonization processes, then the CNFs membranes were functionalized by (6.8 wt.%) HA by the hydrothermal process (130ºC for 90 min). The prepared membranes were in-vitro tested for bioactivity in Simulated Body Fluid (SBF) solution and for biodegradability in Phosphate Buffer Saline (PBS) solution. We have successfully prepared a bioactive and biodegradable membrane by immersing it in SBF and PBS solutions respectively for 14 days, where a bioactive layer of Hydroxy-Carbonated Apatite (HCA) was found on its surface. The formed layer of HCA has been characterized by XRD, FTIR, and SEM. The biodegradability of the membranes has been characterized by FTIR, SEM, and ICP for the PBS solution after different time intervals (1, 3, 5, 7 and 14) days. The membrane of (CNF/6%HA) is more biodegradable than other membranes of (CNF, and CNF/8%HA) (Figure 1).

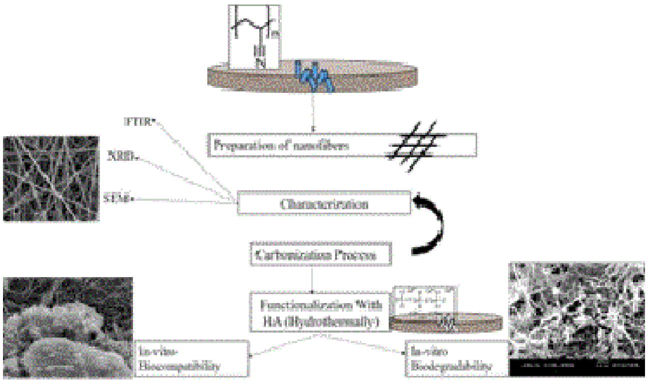

Figure 1: Graphical abstract.

Keywords: Carbon nano fibers; Hydroxyapatite; Bioactivity; Biodegradability

Introduction

There are several conditions in which hurt bone may not be capable of healing itself. In massive traumatic bone loss or primary tumor resection the bone defect may exceed a critical size and will not heal with the help of mechanical fixation alone, which may result in a non-union. For such critical bone sized defects added material is necessary to fill the gap [1]. The current gold standard treatment for these critical-sized defects is autogenous bone grafting. Autogenous bone grafts fulfill three main attributes: they are osteogenic, osteoinductive and osteoconductive.

Osteogenic means that they contain living cells which can differentiate into osteoblasts. Osteoinductive describes the ability to stimulate local or added cells to differentiate into osteoblasts and thereby increase bone healing. Bone grafts also act as scaffolds: on their surface new bone material can be generated (osteoconductive) [2]. The definition of bioactive materials (scaffolds) indicates that strong material / tissue bonding is the key to ensure a high success rate of an implantation. The bioactivity means that a HA-like layer has been formed on the membrane immersed in SBF, which is responsible for the interactions within hard and soft tissues [3]. Bioactive nanomaterials (Scaffolds) have well-defined nanostructures in terms of the size of the material, the shape, the channels, pore structure and the surface domain. They include nanoparticles, nanotubes, nanofibres, nanogels, nanofilms, and nanofoams [4]. Carbon nanofibers with diameters that fall into submicron and nanometer range have attracted growing attention in recent years due to their superior chemical, electrical, and mechanical properties that are combined with their unique 1-D nanostructures

---

***Corresponding author:** Abd El-Aziz A, Department of Fabrication Technology and Department of Materials Science, Alexandria University, Egypt, Tel: 01149431552; E-mail: aabdelaziz@srtacity.sci.eg

Received June 09, 2017; **Accepted** July 05, 2017; **Published** July 11, 2017

Citation: Abd El-Aziz A, El-Maghraby A, Kandil SH (2017) Study of In vitro Bioactivity and Biodegradability of the Hydrothermally Prepared Carbon Nanofibrous/ Hydroxyapatite (Cnf/Ha) Membranes. J Bone Res 5: 176. doi: 10.4172/2572-4916.1000176

[5]. Composite Carbon nanofiber/Hydroxyapatite (CNF/HA) is used to solve bone critical bone sized defects. Hydroxyapatite coatings (HA, $Ca_{10}(PO4)_6(OH)_2$) are used to promote rapid fixation and bone integration of bone orthopedic and dental implants. HA is not only bioactive, but also osteoconductive, non-toxic, non-immunogenic, and its structure is crystallographically similar to that of bone and provides an ideal environment for cells adhesion, proliferation and differentiation [6]. The aim of the present study is to prepare CNFs/HA nanocomposite by the hydrothermal process and to study the in-vitro bioactivity and biodegradability of the prepared membranes for bone regeneration in the case of critical sized bone defects.

Materials and Methods

Materials

Poly acrylonitrile (PAN) was purchased from sigma Aldrich (USA) with average (M wt.=150000 g/mol, d=1.184 g/ml at 25°C), N, N-Dimethyl Formamide (C_3H_7NO) was obtained from El-Goumhouria Company with Mwt=73.10, minimum assay (GC) 99.0%. Sodium hydrogen phosphate dibasic ($Na_2HPO_4.2H_2O$) extra pure, assay: 99.5-101%, was obtained from Sigma Aldrich Labor chemikalin. Potassium dihydrogen phosphate (KH_2PO_4) was purchased from Oxford laboratory, Mumbai, India. Potassium chloride (KCl) was produced from Ranaxy- fine chemicals limited, Okhla Industrial area, assay 99.5%. Sodium Chloride (NaCl) was purchased from Raheja center, Mumbai, assay 99.9%. Sodium bicarbonate ($NaHCO_3$) was purchased from sigma Aldrich, ≥ 99.0%, pH (8.0-8.6). Potassium hydrogen phosphate dibasic ($K_2HPO_4.3H_2O$) was obtained from oxford laboratory reagent (India), min. assay 98%. Magnesium chloride ($MgCl_2.6H_2O$) was purchased from sigma Aldrich, BioXtra, ≥ 99.0% with sulfate as anion traces ≤ 0.002 %. Calcium Chloride ($CaCl_2$) was purchased from sigma Aldrich, ≥ 99.0%, trace metal basis, mp=772°C. Sodium sulfate anhydrous (Na_2SO4) was purchased from El-Nasr pharmaceutical chemicals company with min. assay 99%. (Tris (hydroxymethyl) aminomethane) (CH_2OH) $3CNH_2$)) was purchased from sigma Aldrich, ≥ 99.8%, ACS reagent. All these compounds were used without further purification.

Methods

Electro spinning of poly acrylonitrile (PAN) nano fibers: The different concentrations of PAN solution were (3, 5, 7, 12 wt.%), they were loaded into a plastic syringe (10 mL). The electro spinning apparatus consisted of high voltage supply, a syringe infusion pump and a ground electrode “drum” as collector. The solution was constantly supplied using a syringe pump at a flow rate of 0.5 mL/h, the spinning distance between needle and the ground electrode was fixed to 10 cm with an applied voltage 30 kV.

Preparation of carbon nano fibers (CNFs): The prepared polymeric nanofibrous membranes were thermally treated by stabilization and carbonization processes which have performed using a furnace (Carbolite Tube Furnace) equipped with a tube (60 cm) length and (4 cm) diameter with maximum pressure flow 0.2 bar. The stabilization process was done by heating the prepared polymeric nanofibers at a rate of 1.0°C/min from room temperature to 250°C, and then they were incubated at 250°C for 2 hours at air atmosphere [3]. This was followed by a carbonization step, which took place at 1000°C for 1 hour under Ar gas with heating rate of 5°C/min [7-9].

Functionalization of carbon nano fibers (CNFs) with hydroxyapatite (HA) hydrothermally: The naturally annealed HA, which has been prepared at our labs, it was dispersed in distilled water with two concentrations (6, 8 wt.%). The prepared CNF membranes (30 × 20 mm^2) were immersed in the as-obtained suspension or solution (40 ml), immediately placed into an autoclave and hydrothermally treated for 90 min at 130°C. The resulting samples were left to dry at room temperature and were then placed in a vacuum oven (10 mbar) at 40°C for 72 h prior to further processing [10,11].

***In vitro* bioactivity study:** The bioactivity tests were performed using SBF of pH 7.4, at the temperature of 37°C. Two types of membranes: (1) CNF (control) and (2) CNF/ 6, 8% HA were incubated for 14 days in SBF fluid, in closed polyethylene containers. After 14 days of immersion, the samples were washed with distilled water and then dried at room temperature. The surface morphology and the chemical composition of the samples were examined by SEM, EDX, and FTIR [12].

***In vitro* biodegradation study:** The CNFs membranes were cut into (1 cm × 1 cm) (for each membrane) with an average weight of 3 mg. They were sterilized at an autoclave for 2 h, and were soaked with 5 mL PBS at 37°C in sterile 12-well plates. At predetermined time intervals (1, 3, 5, 7, 14 days), the remaining sample was carefully removed from the well, rinsed using deionized water, dried at 60°C until the mass remained unchanged, and then weighed. The mass loss % was plotted vs. time to get the degradation profile of the membrane [13,14].

Characterization of the prepared materials: Fourier Transmission – IR Spectrophotometer (FTIR -8400S, Shimadzu, Japan) with a resolution of 2 cm^{-1} was used to explore the change in the functional groups before and after the heat treatment and as a result of the bioactivity on SBF functionalization. The samples (5 mg) were mulled with dry potassium bromide (KBr) (20 mg) crystals at room temperature. The spectrum was recorded in the wave number range of 4000-350 cm^{-1} with a resolution of 2 cm^{-1}. To analyze the crystalline structure of the bioactive layer which has been formed as a result of immersion of the nanofibrous membranes on SBF, X-ray diffraction was performed using (X-ray 7000 Shimadzu-Japan) at room temperature. The Bragg angle (2θ) in the range from 10 to 80 degree was measured to determine the degree of crystallinity of the membranes. The X-ray source is a Cu target generated at 30 KV and 30 mA with a scan speed of 4 deg /min. The surface morphology of the electrospun fibers were investigated by the field scanning electron microscopy (SEM, JEOL JSM 6360LA, Japan), with an Electron Dispersive X-Ray unit (EDX). The Inductively Coupled Plasma (ICP) optical emission spectrometry (Agilant Technique 5100 (ICP-OES-VDV), Australia), is an analytical technique what is used for the detection of trace metals. It is a type of emission spectroscopy that uses the inductively coupled plasma to produce excited atoms and ions that emit electromagnetic radiation at wavelengths characteristic of a particular element. It was used to determine the concentration of Ca, and P at the PBS solution after each time interval. High Resolution Transmission Electron Microscope (HR-TEM, Tecnai G20, FEI, and Netherland) was used for the purpose of imaging, crystal structure revelation and elemental analysis “qualitative and semi-quantitative” analysis. Two different modes of imaging were employed; the bright field at electron accelerating voltage 200 kV using lanthanum hexaboride (LaB6) electron source gun and the diffraction pattern imaging. Eagle CCD camera with (4 k × 4 k) image resolution was used to acquire and collect transmitted electron images. TEM Imaging and Analysis (TIA) software was used for the spectrum acquisition and analysis of EDX peaks.

Results and Discussion

Preparation of carbon nano fibers (CNFs)

Figure 2 shows SEM images of the electrospun polymeric nanofibrous membranes that have different concentrations of PAN

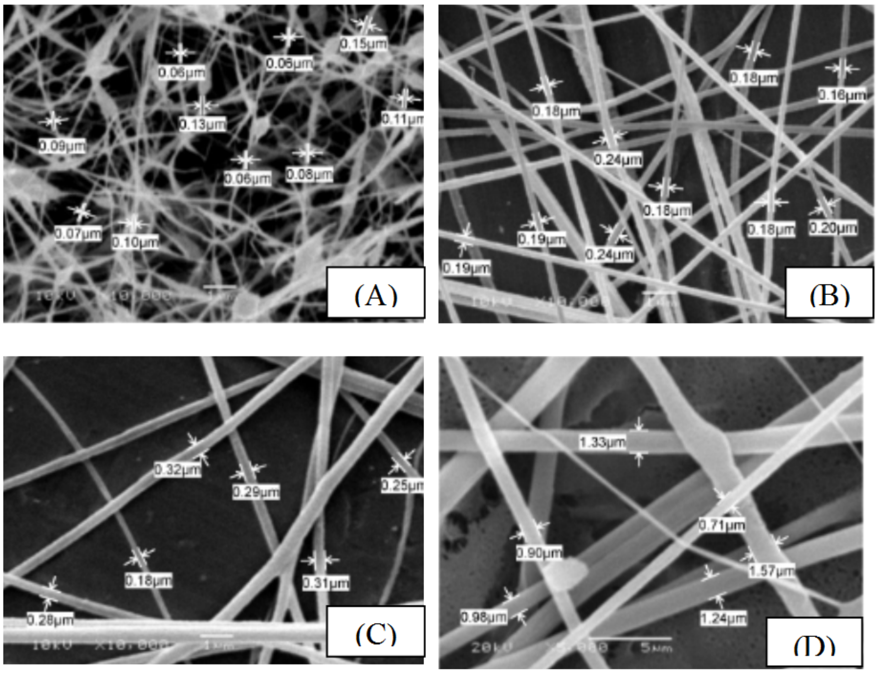

Figure 2: SEM images of the electrospun polymeric nanofibrous membranes.

solutions (3, 5, 7, 12 wt.%). The massive increase in electrostatic repulsion tends to an increase in the surface area and leads to a decrease of the fiber diameters [5,12,15]. The average diameters of the fiber membranes with different concentrations are ranged from 70 nm to 150 nm. Figure 3 shows the difference of the functional groups before and after the heat treatment of the polymeric nanofiber by FT-IR analysis. After the carbonization process, there were notable changes of the characteristic absorption peaks of the samples, the most prominent structural changes were observed. For the polymeric nanofibrous membranes, the strong absorption peak located in the 2260 cm^{-1}, which was characteristic of a nitrile group $C\equiv N$, has completely disappeared after the carbonization process. It has been found that the peak intensity at 2243 cm^{-1} was largely decreased due to the nitrile groups, which was converted to C=N during the cyclization step to form conjugated groups, depending on the extent of the stabilization process [7]. The shoulder like peak at 1000 cm^{-1}, 1500 cm^{-1} are due to the (C=C, C=N, N=H mixed). There are two distinct observations at the following spectra. First, the reaction of nitriles has resulted in a conjugated C=N containing structures of the intermolecular cyclization or intermolecular crosslinking occurring at the stabilization process. Secondly, the generation of conjugated C=C structures that results from dehydrogenation or from imine and amine tautomerization and subsequent isomerization process which takes place at the carbonization stage.

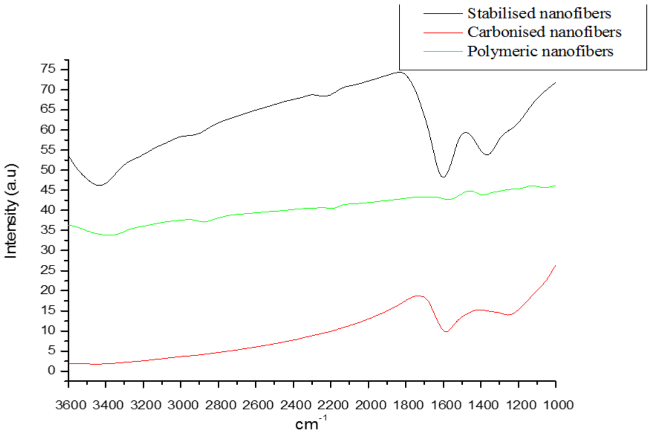

Figure 3: The difference of the functional groups before and after the heat treatment of the polymeric nanofiber by FT-IR analysis.

Functionalization of CNF membranes with HA

Figure 4 shows the high resolution-TEM images of the prepared CNFs membranes after hydrothermal processing. The surfaces of hydrothermal-treated CNFs appear to be amorphous. Furthermore, nanosized pores, serving as the aforementioned nucleation sites, were observed (inset in Figure 4) [11,16]. From the high magnification CNFs image, we found that the diameter of the individual nanofiber has the size 140 nm. Figure 5 shows the SEM micrographs of HA agglomerates in the composite membranes. The HA appears as agglomerates white

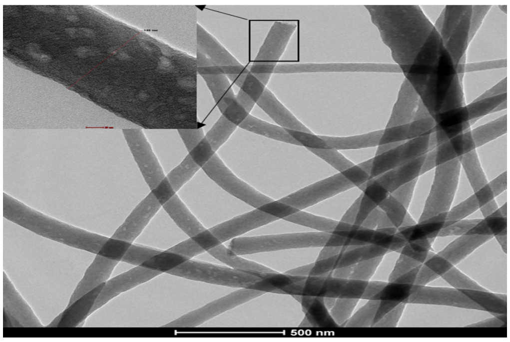

Figure 4: High resolution-TEM images of the prepared CNFs membranes after hydrothermal processing.

dots on the surface of CNFs membrane [9]. In the final stage of the nonwoven membranes production the stabilized mats were carbonized at 1000°C in the inert Argon atmosphere. During carbonization, the carbon content has increased by at least 63 wt.% that is shown in Table 1 and formation of three dimensional carbonaceous structures with different percentages of (Ca, P) elements as a result of HA addition [7,12].

In vitro bioactivity of the CNFs membranes

To observe the role of HA incorporation into the CNF membranes for the formation of apatite-like materials after the incubation in SBF solutions, SEM, XRD, FTIR, and EDX analysis were performed. Figure 6 shows the SEM images of CNF, CNF-6% HA, and CNF-8%HA composite nanofibers before and after immersion into SBF solution for 14 days. However, in the presence of HA into the CNF nanofibers, the formation of apatite-like materials has gradually started and their size which has increased monotonically with increasing the concentration of HA [17]. Figure 6B shows the SEM images taken after 14 days which revealed the intense formation of the apatite-like materials throughout the CNFs membranes. A prolonged immersion of 14 days resulted in dramatic changes in the morphology of the nanofiber; namely, pore spaces were clogged due to considerable crystal growth and overlapping of the spherical crystals [18]. To confirm the formation of apatite-like materials in the CNF mats after immersion into SBF solution, we performed the SEM-EDX analysis. Table 2 shows the atomic weight percent of Ca and P before and after immersion into SBF solution. In case of CNF-6%HA, the percentage of Ca and P have been increased after immersion into SBF solution, which confirms the formation of the apatite layer after immersion into SBF solution. Figure 7 shows the XRD of the CNFs membranes before and after the immersion on the SBF solution. Figure 7A shows that pure CNFs had two broad and weak diffraction peaks at $2\theta=24°$ and 43°, corresponding to the graphitic crystallite planes (002) and (100), respectively [19,20]. However, there is a distinct difference in the peak intensities, which indicates that, the graphitization of the carbon nanofiber / HA structure is lower than the graphitization of the solid carbon nanofiber membranes [21]. The presence of HA on the nanofibrous membranes was not clear by XRD. This may be due to the small percentages of HA utilized in this study for preparation of the CNFs membranes. This may also be due to the amorphous nature of the CNF, which does not allow any such peaks of the HA to appear. This has been previously noted by Kanjwal et al. [22]. The diffraction patterns of all samples after 14 days incubation in the SBF solution showed two clear peaks at 32° and 46° corresponding to the (211) and (222) main reflection planes of apatite-like calcium phosphate (JCPDS No. 09-0432) as shown in Figure 7B. The XRD data clearly confirmed that the apatite was also formed on CNF membranes [17,23,24]. Figure 8A and 8B shows the FTIR of the carbon nanofibrous membranes before and after immersion in the SBF at 37°C for 14 days. It has been found that the peak intensity at 2243 cm^{-1} was largely decreased Figure7A due to the nitrile groups during the cyclization to form conjugated C=N groups 7. There is no obvious difference between the CNF and the membranes modified with HA. However, Figure 8B shows that the band observed at 3417 cm^{-1} is attributed to hydroxyl group (OH) stretching, but the band at 1592 cm^{-1} was attributed to V2 bending mode of the water crystal that were adsorbed on the surface [25,26]. The resonance at 1290 cm^{-1} was attributed to the C-O in the CO_3^{-2} group. The range from 1000-1100 and 590 cm^{-1} corresponded to a calcium phosphate, P-O group [23]. All results indicated that the converted layer might be an amorphous calcium phosphate material that is a precursor to the formation of the crystalline HA phase.

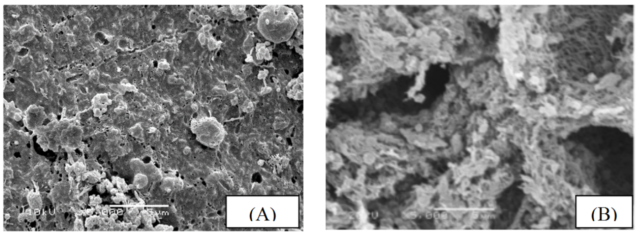

Figure 5: SEM micrographs of HA agglomerates in the composite membranes.

% mass	CNF-6% HA	CNF-8%HA
C	63.36	54.97
O	22.16	23.12
P	5.06	7.33
Ca	9.42	14.58

Table 1: Carbon content increased by 63 wt.% during carbonization.

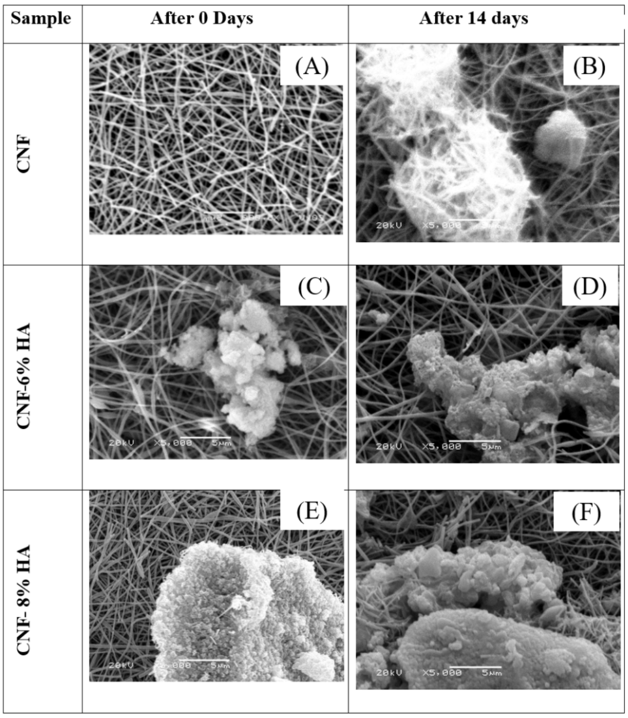

Figure 6: **(A)** SEM images of CNF, CNF-6% HA, and CNF-8%HA composite nanofibers before and after immersion into SBF solution for 14 days; **(B)** SEM images taken after 14 days which revealed the intense formation of the apatite-like materials throughout the CNFs membranes.

Samples	%Atomic	Ca		P		O	
		Before	After	Before	After	Before	After
CNF-6HA		9.42	27.06	5.06	8.58	22.16	38.07
CNF-8HA		14.58	12.48	7.33	6.14	23.12	41.1

Table 2: Atomic weight percent of Ca and P before and after immersion into SBF solution.

In vitro degradability of the prepared membranes

The degradation of the membranes was monitored by incubation in PBS at 37°C. The mass loss percentage of the scaffolds with different time intervals (1, 3, 5, 7, 14 days) is shown on Figure 9; the mass loss

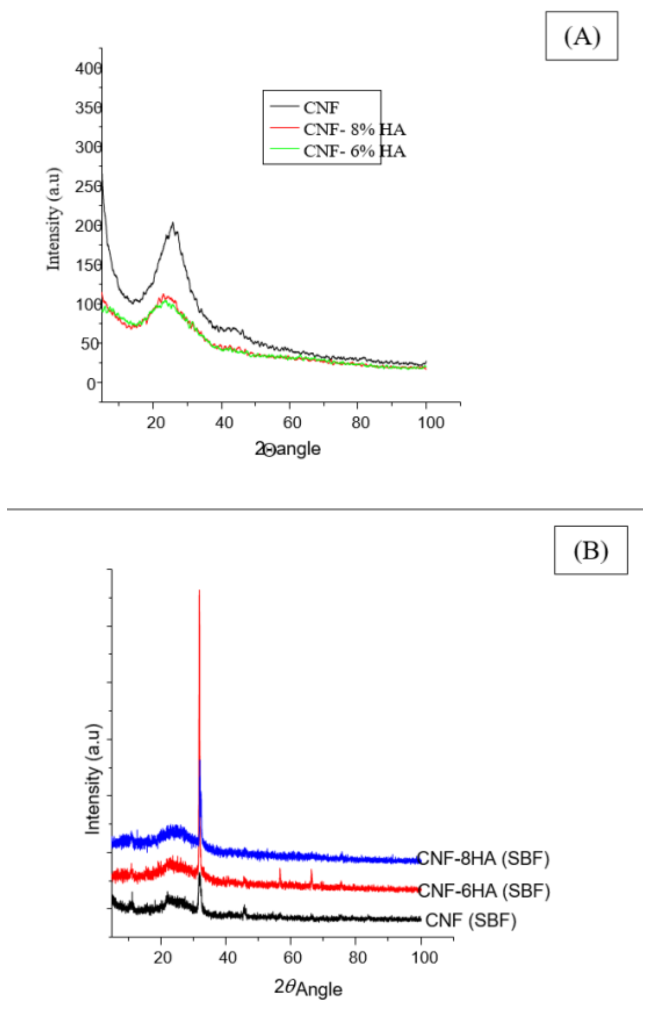

Figure 7: XRD of the CNFs membranes before and after the immersion on the SBF solution. **(A)** Pure CNFs had two broad and weak diffraction peaks at $2\theta=24^\circ$ and 43; **(B)** Diffraction patterns of all samples after 14 days incubation in the SBF solution.

percentage has been calculated using the following equation:

$$WL = (wi - wt)/wi \times 100$$

Where WL is the mass loss percentage of sample, and wi is the initial weight of the dry sample, wt is the weight of dry sample at any given time (1, 3, 5, 7, 14 days). The CNF and CNF/8HA have the strongest resistance to degradation as they held their initial weight after two weeks. In case of the CNF/6HA, the mass loss percentages have been decreased with the time intervals until the 7th day. After this period the degradation percentage has been constant and reached 20 wt.% of their initial weight. After 14 days' incubation in PBS, most of the fibers were swollen and part of fibers was broken down as shown on Figure 10; this was ascribed to the chain relaxation of the fibers in the medium and the hydrolytic cleavage of the chains 27. A small number of micro-cracks and voids were observed on the nanofiber surface. The surface roughness has increased and fiber fractures were present, unlike that in the samples before. The smaller fiber diameters of the scaffolds can increase the surface to volume ratio of the scaffold and increase the rate of degradation that has been shown on Table 2 in case of CNF-6HA 28. Table 3 shows the change in the ion concentrations of Ca, P on the PBS medium of the different incubation time for 14 days, as measured by means of (ICP- OES-VDV). For comparing between 3 samples (CNF, CNF-6HA, and CNF-8%HA), the Ca and P concentrations, which have been released from the samples were monitored. This has increased with increasing the percentages of HA. The releasing of Ca and P from

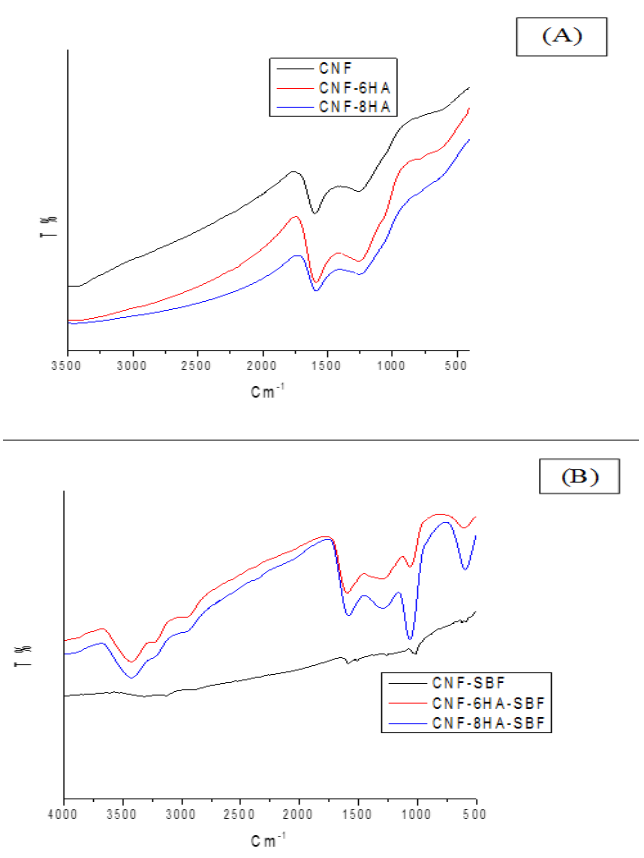

Figure 8 (A, B): FTIR of the carbon nanofibrous membranes before and after immersion in the SBF at 37°C for 14 days.

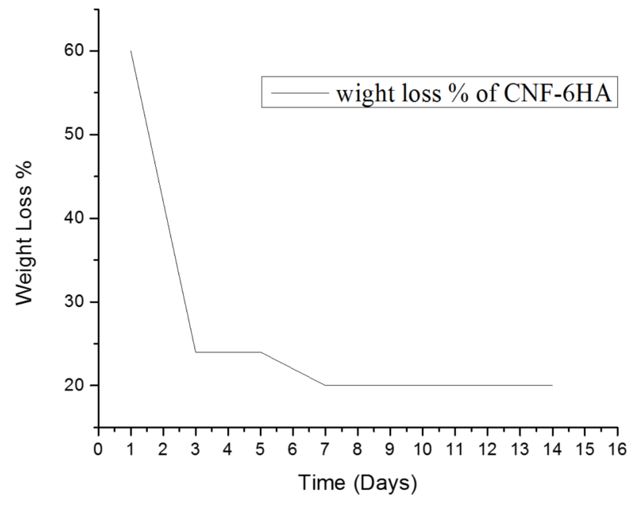

Figure 9: Mass loss percentage of the scaffolds with different time intervals (1, 3, 5, 7, 14 days).

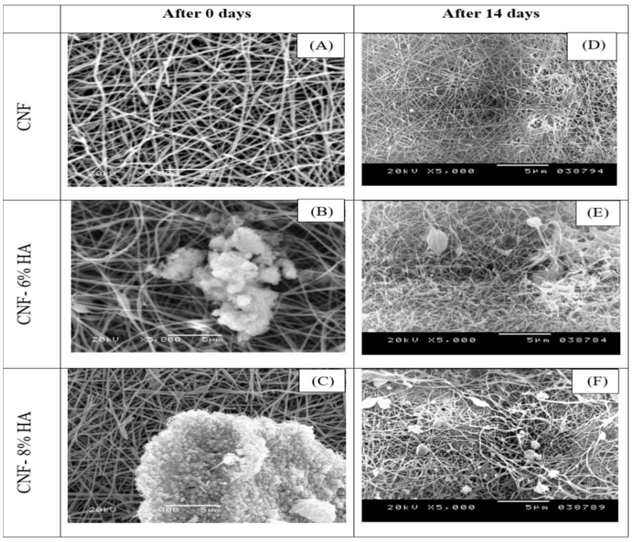

Figure 10: After 14 days incubation in PBS, fibers were swollen and part of fibers was broken down.

PBS control solution contains (Ca=8.494 ppm & P=330.130 ppm).					
After 0 Day			After 14 days		
Material	Ca	P	Material	Ca	P
CNF	22.57	304.7	CNF	22.07	395.37
CNF-6%HA	16.92	337.25	CNF-6%HA	30	340
CNF-8%HA	21.356	308.58	CNF-8%HA	23.95	342.74

Table 3: Change in the ion concentrations of Ca, P on the PBS medium at different incubation time for 14 days.

the modified membranes is due to the degradation of HA 29. The mechanism of the HA degradation in the PBS medium is as follows.

Conclusions

- The functionalization of CNFs with hydroxyapatite (HA) did not cause any change in the average diameter of the CNFs in addition to the agglomeration of HA which appeared as white dots on the fiber threads.
- The *in vitro* bioactivity and biodegradability results demonstrated that CNF, which was modified with 6% HA was a more biodegradable membrane than other membranes. The membranes that were modified by HA (CNF-6HA, and CNF-8%HA) proved to be more bioactive than the CNF membrane without modification with HA.

Acknowledgment

We thank the Science and Technology Development Fund STDF for the fund of this project No. (11949) under the title of (Preparation and characterization of Carbon Nano fiber (CNF) / Hydroxyapatite (HA) nanocomposite for biomedical application), through the call STDF-Short Term Fellowship (STF).

References

1. De P, Ludeña D (2013) Cell culture in autologous fibrin scaffolds for applications in tissue engineering. Exp Cell Res 322: 1-11.
2. Lichte P, Pape HC, Pufe T, Kobbe P, Fischer H (2011) Scaffolds for bone healing: concepts, materials and evidence. Injury 42: 569-573.
3. Chen IH, Wang CC, Chen CY (2010) Fabrication and characterization of magnetic cobalt ferrite/polyacrylonitrile and cobalt ferrite/carbon nanofibers by electrospinning. Carbon NY 48: 604-611.
4. Zhao X, Courtney JM, Qian H (2011) Bioactive Materials in Medicine.
5. Zhang L, Aboagye A, Kelkar A, Lai C, Fong H (2013) A review: carbon nanofibers from electrospun polyacrylonitrile and their applications. J Mater Sci 49: 463-480.
6. Xiaoying L, Yongbin F, Dachun G, Wei C (2007) Preparation and Characterization of Natural Hydroxyapatite from Animal Hard Tissues. Eng Mater 343: 213-216.
7. Cho CW, Cho DH, Ko YG, Kwon OH, Kang IK (2007) Stabilization, Carbonization, and Characterization of PAN Precursor Webs Processed by Electrospinning Technique. Carbon Lett 8: 313-320.
8. Rahaman MS a, Ismail a. F, Mustafa A (2007) A review of heat treatment on polyacrylonitrile fiber. Polym Degrad Stab 92: 1421-1432.
9. Yamashita Y, Aoki N (2008) Carbonization conditions for electrospun nanofibre of polyacylonitrile copolymer. Indian J Fibre Text Res 33: 345-353.
10. Abdal-hay A, Vanegas P, Hamdy AS, Engel FB, Lim JH (2014) Preparation and characterization of vertically arrayed hydroxyapatite nanoplates on electrospun nanofibers for bone tissue engineering. Chem Eng J 254:612-622.
11. Chuang CM, Huang CW, Teng H, Ting JM (2012) Hydrothermally synthesized RuO2/Carbon nanofibers composites for use in high-rate supercapacitor electrodes. Compos Sci Technol 72: 1524-1529.
12. Rajzer I, Kwiatkowski R, Piekarczyk W, Biniaś W, Janicki J (2012) Carbon nanofibers produced from modified electrospun PAN/hydroxyapatite precursors as scaffolds for bone tissue engineering. Mater Sci Eng C 32: 2562-2569.
13. Hanani F, Shahitha F, Hussain J (2014) In vitro degradation study of novel HEC / PVA / collagen nano fibrous scaffold for skin tissue engineering applications. Polym Degrad Stab 110: 473 481.
14. Shi R, Xue J, He M, Chen D, Zhang L, Tian W (2014) Structure , physical properties , biocompatibility and in vitro/vivo degradation behavior of anti-infective polycaprolactone-based electrospun membranes for guided tissue / bone regeneration. Polym Degrad Stab 109: 293-306.
15. Liao S, Chan CK, Ramakrishna S (2010) Electrospun nanofibers Work for medicine? Front Mater Sci China 4: 29-33.
16. Chen H, Jiang G, Yu W, Liu D, Liu Y, et al. (2016) Electrospun carbon nanofibers coated with urchin-like ZnCo2O4 nanosheets as a flexible electrodematerial. J Mater Chem A 4: 5958-5964.
17. Nirmala R, Nam KT, Park DK, Woo-il B, Navamathavan R, et al. (2010) Structural, thermal, mechanical and bioactivity evaluation of silver-loaded bovine bone hydroxyapatite grafted poly(ε-caprolactone) nanofibers via electrospinning. Surf Coatings Technol 205: 174-181.
18. Noh KT, Lee HY, Shin US, Kim HW (2010) Composite nanofiber of bioactive glass nanofiller incorporated poly(lactic acid) for bone regeneration. Mater Lett 64: 802-805.
19. Fu J, Qiao H, Li D, Luo L, Chen K, Wei Q (2014) Laccase Biosensor Based on Electrospun Copper/Carbon Composite Nanofibers for Catechol Detection. Sensors (Basel) 14: 3543-3556.
20. Iyuke SE, Simate GS (2008) Synthesis of Carbon Nanomaterials in a Swirled Floating Catalytic Chemical Vapour Deposition Reactor for Continuous and Large Scale Production. Carbon Nanotub Appl pp: 35-57.
21. El-deen AG, Barakat NAM, Khalil A (2014) Hollow carbon nanofibers as an effective electrode for brackish water desalination using the capacitive deionization process 38: 198-205.
22. Kanjwal MA, Sheikh FA, Nirmala R, Macossay J, Kim HY (2011) Fabrication of poly(caprolactone) nanofibers containing hydroxyapatite nanoparticles and their mineralization in a simulated body fluid. Fibers Polym 12: 50-56.
23. Deliormanl AM (2013) Size-dependent degradation and bioactivity of borate bioactive glass. Ceramics International 39: 8087-8095.
24. Mohan A, Gandhi M, Swamiappan S (2014) In-vitro bioactivity studies of chitin/diopside composites. Int J Chem Tech Res 6: 3993-3995.
25. Lak A, Mazloumi M, Mohajerani MS, Zanganeh S, Shayegh MR, et al. (2008) Rapid Formation of Mono-Dispersed Hydroxyapatite Nanorods with Narrow-Size Distribution via Microwave Irradiation. J Am Ceram Soc 91: 3580-3584.

26. Mohandes F, Salavati-Niasari M, Fathi M, Fereshteh Z (2014) Hydroxyapatite nanocrystals: Simple preparation, characterization and formation mechanism. Materials Science and Engineering: C 45:29-36.

27. Liu Y, Cui H, Zhuang X, Wei Y, Chen X (2014) Electrospinning of aniline pentamer-graftgelatin/PLLA nanofibers for bone tissue engineering. Acta Biomater 12:5074-5080.

28. Mansourizadeh F, Shahabi F, Mansourizadeh F, Pasban E (2014) In vitro degradation of electrospinning PLLA/HA nanofiber scaffolds compared with pure PLLA 4:330-334.

29. Kim HW, Lee HH, Chun GS (2008) Bioactivity and osteoblast responses of novel biomedical nanocomposites of bioactive glass nanofiber filled poly(lactic acid). J Biomed Mater Res. 85: 651-663.